Dyotropic Rearrangement of Organosilylenium Ions in the Gas Phase

R. Bakhtiar, C. M. Holznagel, and D. B. Jacobson*

Department of Chemistry, North Dakota State University, Fargo, North Dakota 58105-5516

Received September 9, 1992

The mechanism of ethene extrusion for unimolecular dissociation of $(CH_3)_3Si^+$ in the gas phase has been studied by using Fourier transform mass spectrometry (FTMS). Collision-activated dissociation (CAD) combined with isotopic exchange reactions suggest that $(CH_3)_3Si^+$ (**4**) and $(C_2H_5)(CH_3)SiH^+$ (**2**) interconvert upon activation. We propose that **2** and **4** interconvert by a concerted 1,2-hydrogen/1,2-methyl migration (dyotropic rearrangement, transition state **3**). We envision that the dyotropic rearrangement involves a thermally allowed $[\sigma_s^2 + \sigma_a^2]$ process. Ethene extrusion from activated **4** proceeds by initial rearrangement to **2** followed by β-hydrogen migration with ethene elimination. Isotopic labeling studies suggest that $(CH_3)_2SiH^+$ decomposes by a similar mechanism with initial rearrangement to $(C_2H_5)SiH_2^+$ by a concerted 1,2-hydrogen/1,2-methyl migration. Subsequent decomposition by β-hydrogen migration/ethene elimination then yields SiH_3^+. In contrast to the above rearrangements, activated $(C_2H_5)(CH_3)_2Si^+$ eliminates ethene by direct β-hydrogen migration (no isomerization) and was confirmed by labeling studies. It is argued that the corresponding dyotropic rearrangements for $(C_2H_5)(CH_3)_2Si^+$ (processes 16 and 17) have prohibitive barriers; consequently, β-hydrogen migration with ethene elimination is observed directly.

Introduction

Cationic and anionic organosilane species are highly reactive in the gas phase[1-4] with a number of interesting facile rearrangements being observed. For example, collision-activated dissociation (CAD)[5] of $(CH_3)_3Si^+$ yields predominant elimination of ethene (process 1).[6,7] CAD of

$$(CH_3)_3Si^+ \xrightarrow{CAD} (CH_3)SiH_2^+ + C_2H_4 \qquad (1)$$

the $(C_2H_5)(CH_3)SiH^+$ isomer yields an analogous dissociation; consequently, CAD is not structurally diagnostic for simple alkylsilylenium ions.[7] The elimination of ethene from $(CH_3)_3Si^+$ is obviously a complex reaction and may proceed by prior rearrangement to an ethylmethylsilylenium ion (process 2) prior to ethene elimination. Alternatively, ethene elimination from $(CH_3)_3Si^+$ may proceed by simple extension of vibrations (process 3). In any case, elimination of ethene from *activated* $Si(CH_3)_3^+$ is a facile process.

$$[(CH_3)_3Si^+]^* \rightarrow (CH_3CH_2)(CH_3)SiH^+ \qquad (2)$$

In this report we use specific ion/molecule reactions involving isotopically labeled reagents combined with CAD to study the mechanism of ethene elimination from

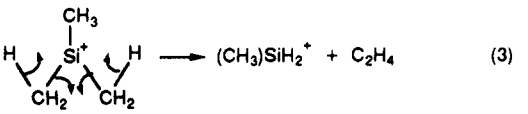

(3)

$(CH_3)_3Si^+$. Our results provide evidence for a facile dyotropic rearrangement[8] involving the interconversion of activated $(CH_3)_3Si^+$ and $(C_2H_5)(CH_3)SiH^+$ in the gas phase.

Experimental Section

All experiments were performed by using a modified Nicolet FTMS-1000 Fourier transform mass spectrometer[9,10] equipped with a 5.08-cm cubic trapping cell and 3.0-T superconducting magnet.[11] A Bayard/Alpert type ionization gauge was used to monitor pressure and was calibrated by using reactions with well-known rate constants. The pressure of reagent neutrals was subsequently corrected by using ionization cross sections.[12] Absolute pressure uncertainties are believed to be <30% with relative uncertainties <10%. $(CH_3)SiD_3$ and $(CH_3)_2SiD_2$ were synthesized by reduction of the corresponding chloride with LAD (lithium aluminum deuteride)[13] and purified by vacuum distillation. Ethene-d_4 and ethene-$^{13}C_2$ were obtained from MSD Isotopes with >98% isotopic purity. All other reagents were used as supplied, except for multiple freeze-pump-thaw cycles to remove noncondensable gases.

Specific organosilylenium ions were generated by electron impact ionization of appropriate precursor organosilanes. For example, $(CH_3)SiH_2^+$ was formed from $(CH_3)SiH_3$, $(CH_3)SiD_2^+$

* To whom correspondence should be addressed.

(1) Oppenstein, A.; Lampe, F. W. In *Review of Chemical Intermediates*; Strausz, O. P., Ed.; Elsevier: Amsterdam, 1986; Vol. 6, p 275.
(2) Schwarz, H. In *The Chemistry of Organic Silicon Compounds*; Patai, S. Rapport, Z., Eds.; Wiley: New York, 1989; p 445.
(3) DePuy, C. H.; Damrauer, R.; Bowie, J. H.; Sheldon, J. C. *Acc. Chem. Res.* **1987**, *20*, 127.
(4) Bowie, J. H. *Mass Spectrom. Rev.* **1984**, *3*, 1.
(5) (a) Cooks, R. G. *Collision Spectroscopy*; Plenum Press: New York, 1978. (b) *Tandem Mass Spectrometry*; McLafferty, F. W., Ed.; Wiley: New York, 1983. (c) Busch, K. L.; Glish, G. L.; McLuckey, S. A. *Mass Spectrometry/Mass Spectrometry*; VCH: New York, 1988.
(6) Groenewold, G. S.; Gross, M. L. *J. Organomet. Chem.* **1982**, *235*, 165.
(7) Holznagel, C. M.; Bakhtiar, R.; Jacobson, D. B. *J. Am. Soc. Mass Spectrom.* **1991**, *2*, 278.
(8) Reetz, M. T. *Adv. Organomet. Chem.* **1977**, *16*, 33.
(9) For reviews on FTMS, see: (a) Gross, M. L.; Rempel, D. L. *Science (Washington, D.C.)* **1984**, *226*, 26. (b) Wanczek, K.-P. *Int. J. Mass Spectrom. Ion. Proc.* **1989**, *95*, 1. (c) Marshall, A. G. *Acc. Chem. Res.* **1985**, *18*, 316. (d) Comisarow, M. B. *Anal. Chim. Acta* **1985**, *178*, 1. (e) Nibbering, N. M. M. *Acc. Chem. Res.* **1990**, *23*, 279. (f) Marshall, A. G.; Grosshans, P. B. *Anal. Chem.* **1991**, *63*, 215A.
(10) *Fourier Transform Mass Spectrometry*; Buchanan, M. V., Ed.; American Chemical Society: Washington, DC, 1987.
(11) Jacobson, D. B. *J. Am. Chem. Soc.* **1989**, *111*, 1626.
(12) Bartmess, J. E.; Geordiadis, R. M. *Vacuum* **1983**, *33*, 149.
(13) Gaspar, P. P.; Levy, C. A.; Adair, G. M. *Inorg. Chem.* **1970**, *9*, 1272.

0276-7333/93/2312-0880$04.00/0

from $(CH_3)SiD_3$, $(CH_3)_2SiH^+$ from $(CH_3)_2SiH_2$, $(C_2H_5)(CH_3)SiH^+$ from $(C_2H_5)(CH_3)SiH_2$, etc. All precursor organosilanes were introduced into the vacuum chamber via a pulsed solenoid inlet valve[14] in order to prevent complicating side reactions with background organosilane.[1-4] The pulsed valve was triggered off the quench pulse with the valve duration varied (typically between 2 and 3 ms) in order to control the amount of pulsed reagents. The ballast pressure in the pulsed valve assembly was <1 Torr. Electron impact ionization (typically 50–100 ms beam duration, −70 eV) occurs 50 ms after triggering the pulsed valve. A variable delay following ionization (ca. 1 s) was employed to allow the pulsed organosilane reagent to be removed from the vacuum chamber followed by isolation of the desired ions by swept ejection pulses.[9,10] The isolated ions were subsequently allowed to react with a static pressure of specific reagents or were dissociated by collisional-activated dissociation (CAD).[5] A static pressure of 1×10^{-5} Torr of Ar was maintained throughout these experiments and served both to facilitate ion thermalization prior to reaction and as the target for collision-activated dissociation (CAD).[5]

Details for CAD in conjunction with FTMS have been described elsewhere.[15] CAD breakdown curves were obtained by varying the kinetic energy of the ions (typically between 1 and 100 eV) by adjusting the duration of the CAD electric field pulse (typically between 100 and 600 μs). The maximum kinetic energy acquired by an irradiated ion (in excess of thermal energy) was calculated by using the relationship

$$E_{tr(max)} = (E_{Rf})^2 e^2 t^2 / 8m \qquad (4)$$

where E_{Rf} is the electric field amplitude, e is the electric charge, t is the duration of the electric field pulse, and m is the mass of the ion.[16,17] CAD fragment ion intensities are plotted as a fraction of the initial parent ion intensity (no excitation) versus kinetic energy. This allows both the energy dependency for fragmentation and the fragmentation efficiency to be compared directly for related systems. CAD breakdown curves are reproducible with <3% absolute variation in ion abundances for replicate curves. The spread in ion kinetic energy is dependent on the total average kinetic energy and is 65% at 1 eV, 19% at 10 eV, 11% at 30 eV, and 6% at 100 eV.[18]

In addition to conventional FTMS-CAD, CAD by using sustained "off-resonance" irradiation (SORI) for ion activation was investigated where the translational energy of an irradiated ion is given by

$$E_{tr} = \{(E_{Rf})^2 e^2 / [2m(\omega - \omega_c)^2]\} \sin^2[(\omega - \omega_c)t/2] \qquad (5)$$

where ω (rad s^{-1}) is the excitation frequency and ω_c is the natural cyclotron frequency of the ion.[16] A consequence of "off-resonance" irradiation is that an ion undergoes acceleration–deceleration cycles throughout the duration of the electric field pulse. Hence, ions can be irradiated for an extended period while a low *maximum* translational energy is maintained. When a long-duration (500-ms) "off-resonance" electric field pulse and an appropriate $\Delta\omega$ ($\Delta\omega = \omega - \omega_c$) are employed, an ion can be slowly collisionally activated by sequential, inelastic collisions prior to fragmentation.[19] This activation technique (SORI-CAD) is analogous to infrared multiphoton dissociation (IRMPD) for probing the lowest energy pathway for ion dissociation.[20] The lowest energy pathway for dissociation of ions was studied by using SORI-CAD, employing a 500-ms electric field pulse and appropriate $\Delta\omega$.

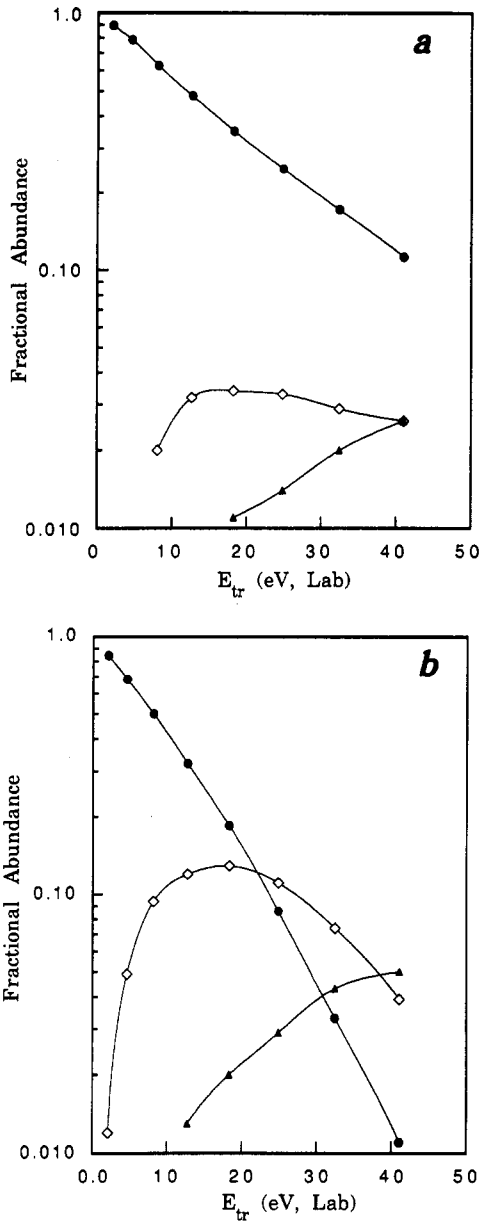

Figure 1. Variation of fractional ion abundances as a function of kinetic energy (laboratory frame) for "on-resonance" irradiation for CAD of $C_3H_9Si^+$ isomers (trapping voltage 1.2 V) $(CH_3)_3Si^+$ (a) and $(C_2H_5)(CH_3)SiH^+$ (b): (●) $C_3H_9Si^+$; (◇) CH_5Si^+; (▲) CH_3Si^+.

Results and Discussion

CAD of $C_3H_9Si^+$ Isomers. The CAD breakdown curves for $(CH_3)_3Si^+$ and $(C_2H_5)(CH_3)SiH^+$ are illustrated in Figure 1. Both $C_3H_9Si^+$ ions yield identical fragmentations with C_2H_4 elimination dominating (process 6). At high

$$C_3H_9Si^+ \rightarrow CH_5Si^+ + C_2H_4 \qquad (6)$$

kinetic energy some CH_3Si^+ is also observed. MS/MS/MS[21] revealed that CH_3Si^+ is formed primarily by sequential C_2H_4/H_2 loss instead of by direct C_2H_6 elimination. These results are in agreement with a high-energy

(14) A detailed description of pulsed valve introduction of reagent gases in conjunction with FTMS can be found in: Carlin, T. J.; Freiser, B. S. *Anal. Chem.* **1983**, *55*, 571.

(15) For discussions of CAD involving FTMS, see: (a) McIver, R. T., Jr.; Bowers, W. D. In *Tandem Mass Spectrometry*; McLafferty, F. W., Ed.; Wiley: New York, 1983; p 287. (b) Cody, R. B.; Burnier, R. C.; Freiser, B. S. *Anal. Chem.* **1982**, *54*, 96. (c) Burnier, R. C.; Cody, R. B.; Freiser, B. S. *J. Am. Chem. Soc.* **1982**, *104*, 7436. (d) Jacobson, D. B.; Freiser, B. S. *J. Am. Chem. Soc.* **1983**, *105*, 736, 7484.

(16) Beauchamp, J. L. *Annu. Rev. Phys. Chem.* **1971**, *22*, 527.

(17) It has been suggested that the kinetic energy obtained by an irradiated ion is much less than that calculated from eq 4: Grosshans, P. B.; Shields, P.; Marshall, A. G. *J. Am. Chem. Soc.* **1990**, *112*, 1275.

(18) Comisarow, M. B. *J. Chem. Phys.* **1971**, *55*, 187.

(19) Gauthier, J. W.; Trautman, T. R.; Jacobson, D. B. *Anal. Chim. Acta* **1991**, *246*, 211.

(20) Thorne, L. R.; Beauchamp, J. L. In *Gas Phase Ion Chemistry*; Bowers, M. T., Ed.; Academic Press: New York, 1984; Vol. 3, p 41.

(21) Cody, R. B.; Burnier, R. C.; Cassady, C. J.; Freiser, B. S. *Anal. Chem.* **1982**, *54*, 2225.

Table I. Thermochemical Data for Organosilicon Ions Used for Potential Energy Surfaces

ion	ΔH_f[a]	ion	ΔH_f[a]
$(CH_3)SiH_2^+$	204[b]	$(C_2H_5)_2(CH_3)Si^+$	137[c]
$(CH_3)_2SiH^+$	172[b]	$(i\text{-}C_3H_7)(CH_3)SiH^+$	160[c]
$(CH_3)_3Si^+$	147[b]	$(C_2H_4)(CH_3)SiH_2^+$	197[d]
$(C_2H_5)(CH_3)SiH^+$	167[c]	$(C_2H_4)(CH_3)_2SiH^+$	165[d]
$(C_2H_5)(CH_3)_2Si^+$	142[c]	$(C_2H_4)(C_2H_5)(CH_3)SiH^+$	160[d]

[a] In kcal/mol. [b] From ref 22. [c] Estimated by using the known ΔH_f values of the corresponding methylsilylenium ions[22] and assumed energy increments for replacing methyl with ethyl or isopropyl.[24] [d] Calculated by assuming the binding energy of ethene to the silylenium ion is 20 kcal/mol[34,35] and using auxiliary thermochemical information from ref 44.

CAD study of $(CH_3)_3Si^+$.[6] Although both $C_3H_9Si^+$ isomers yield identical fragmentations, there are differences in both the overall fragmentation efficiency and energy dependency. The higher energy required for fragmentation of $(CH_3)_3Si^+$ is due, in part, to its increased thermodynamic stability over $(C_2H_5)(CH_3)SiH^+$ (ca. 20 kcal/mol) (Table I).[22,23]

The lowest energy decomposition pathway for the $C_3H_9Si^+$ isomers was investigated by using SORI-CAD.[19] Both $C_3H_9Si^+$ isomers yield *exclusive* C_2H_4 elimination (process 6), indicating that it is the lowest energy pathway for decomposition. The variation of the fractional abundance of fragment ions for SORI-CAD with a 1.02 V electric field and 1×10^{-5} Torr of Ar as a function of the *maximum* ion kinetic energy (calculated directly from eq 5) for CAD of the $C_3H_9Si^+$ isomers is illustrated in Figure 2. The onset of fragmentation for SORI-CAD is a sensitive function of the amount of internal energy required to dissociate isomeric ions.[19] Figure 2 clearly indicates that more energy is required to extrude ethene from $(CH_3)_3Si^+$ than from $(C_2H_5)(CH_3)SiH^+$.

Ion/Molecule Reactions. Additional insight into the mechanism for C_2H_4 elimination from decomposition of $(CH_3)_3Si^+$ is obtained by studying isotopic exchange involving reaction of $(CH_3)SiH_2^+$, $(CH_3)SiD_2^+$, $(CH_3)_2SiH^+$, and $(C_2H_5)(CH_3)SiH^+$ with isotopically labeled ethene (ethene-d_4 and ethene-$^{13}C_2$). Ethene-d_4 undergoes an exclusive, *single* H/D exchange with $(CH_3)_2SiH^+$ (process 7) (k_{obsd} = [5.2(1.6)] × 10^{-10} cm^3 molecule^{-1} s^{-1}; eff =

$$(CH_3)_2SiH^+ + C_2D_4 \rightarrow (CH_3)_2SiD^+ + C_2D_3H \quad (7)$$

0.47).[25-27] Figure 3 clearly illustrates that a single H/D exchange is observed for reaction with ethene-d_4. Authentic $(CH_3)_2SiD^+$ and $(CH_3)_3Si^+$ are inert toward ethene-d_4 and ethene-$^{13}C_2$. This result indicates that the methyl hydrogens are not involved in the exchange reaction (process 7).

$(C_2H_5)(CH_3)SiH^+$ yields exclusive thermoneutral displacement of an unlabeled ethene with ethene-$^{13}C_2$ (reaction 8) (k_{obsd} = [3.5(1.1)] × 10^{-10} cm^3 molecule^{-1} s^{-1}; eff = 0.33).[7] The product of reaction 8 is inert toward ethene-

$$(C_2H_5)(CH_3)SiH^+ + {}^{13}C_2H_4 \rightarrow ({}^{13}C_2H_5)(CH_3)SiH^+ + C_2H_4 \quad (8)$$

$^{13}C_2$. Six exchangeable hydrogens are observed for reaction of ethene-d_4 with $(C_2H_5)(CH_3)SiH^+$ (process 9) (k_{obsd} =

$$(C_2H_5)(CH_3)SiH^+ \xrightarrow{C_2D_4} (C_2D_5)(CH_3)SiD^+ \quad (9)$$

[4.8(1.4)] × 10^{-10} cm^3 molecule^{-1} s^{-1}; eff = 0.47). Figure 4 clearly demonstrates that only six hydrogen atoms are exchangeable for $(C_2H_5)(CH_3)SiH^+$. The above isotopic exchange reactions presumably proceed by reversible ethene insertion/β-hydrogen migration (process 10).[28-32]

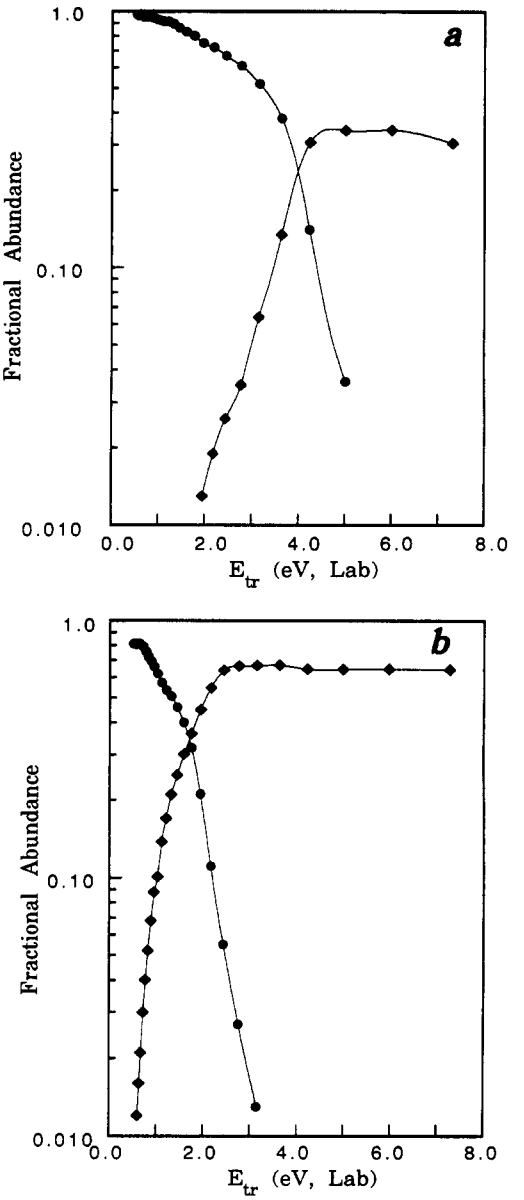

Figure 2. Variation of fractional ion abundances as a function of maximum kinetic energy (calculated directly from eq 5) for "off-resonance" irradiation (500 ms duration pulse, 1.02 V electric field, trapping voltage 1.2 V) for CAD of $(CH_3)_3Si^+$ (a) and $(C_2H_5)(CH_3)SiH^+$ (b): (●) $C_3H_9Si^+$; (◆) CH_5Si^+.

(22) Shin, S. K.; Beauchamp, J. L. *J. Am. Chem. Soc.* **1989**, *111*, 900.
(23) ΔH_f values of ethyl- and isopropylsilylenium ions are estimated by using the known ΔH_f values of the corresponding methylsilylenium ion[22] and assumed energy increments for replacing methyl with ethyl or isopropyl.[24] Auxiliary therochemical information is from ref 44.
(24) Benson, S. W. *Thermochemical Kinetics*; Wiley-Interscience: New York, 1976.
(25) Reuter, K. A.; Jacobson, D. B. *Organometallics* **1989**, *8*, 1126.
(26) k_{obsd} is the experimental rate constant. Uncertainties in reaction rate constants are given in parentheses and are primarily a consequence of pressure uncertainties.
(27) Reaction efficiency (eff) is taken as the ratio of the experimental rate constant to the collision rate constant (i.e., k_{obsd}/k_{coll}). Collision rate constants were calculated by using the Langevin pure polarization theory for nonpolar neutrals (Su, T.; Bowers, M. T. In *Gas Phase Ion Chemistry*; Bowers, M. T., Ed.; Academic Press: New York, 1979; Vol. 1, Chapter 3).
(28) Abernathy, R. N.; Lampe, F. W. *J. Am. Chem. Soc.* **1981**, *103*, 2573.
(29) Barton, T. J.; Tillman, N. *J. Am. Chem. Soc.* **1987**, *109*, 6711.

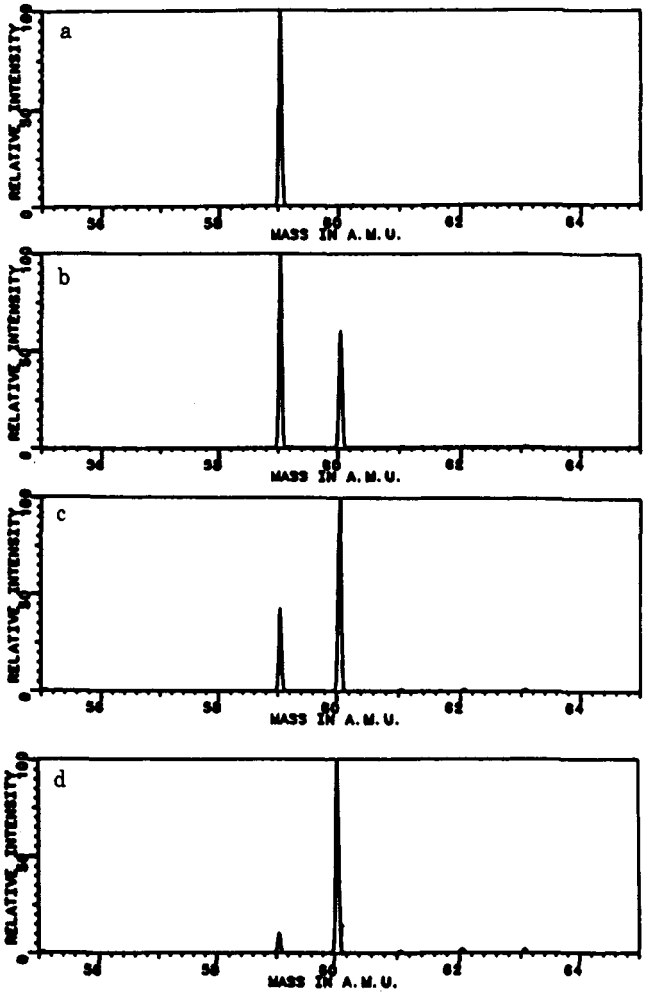

Figure 3. Mass spectra for reaction of $(CH_3)_2SiH^+$ with 2.6 × 10^{-8} Torr of C_2D_4: (a) isolation of $(CH_3)_2SiH^+$ (m/z 59), formed by electron impact ionization of $(CH_3)_2SiH_2$ (pulsed into the vacuum chamber); (b) 1.0-s reaction with C_2D_4; (c) 2.5-s reaction with C_2D_4; (d) 5.0-s reaction with C_2D_4.

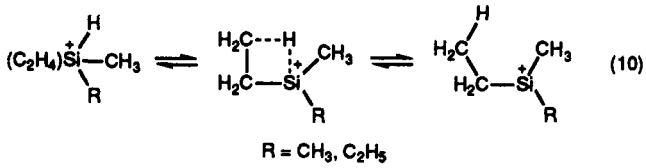

(10)

R = CH_3, C_2H_5

This process (olefin insertion/β-hydrogen migration) is ubiquitous for transition-metal systems where the transition state employs a near-zero M–C–C–H dihedral angle.[33] There are no restrictions in the corresponding organosilane ions from achieving this favorable geometry. The energy of the ethene–silylenium ion collision complex (ca. 20–25 kcal/mol)[34,35] drives the above isotopic exchanges. The silylenium ions in process 10 are estimated to be significantly (ca. 23 kcal/mol) more stable than the corresponding ethene complexes (Table I). The facility

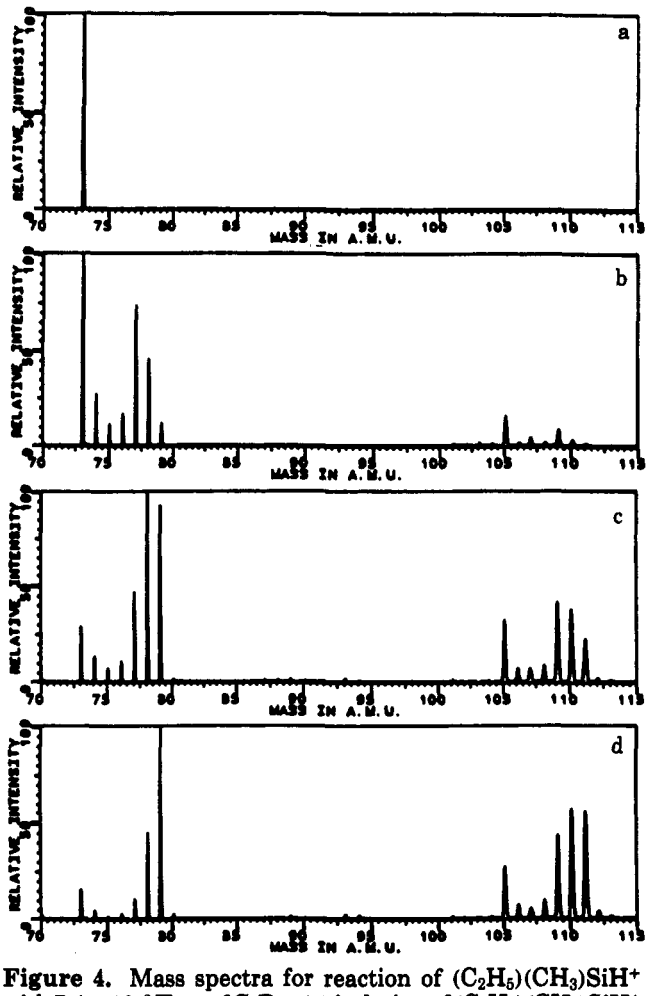

Figure 4. Mass spectra for reaction of $(C_2H_5)(CH_3)SiH^+$ with 7.4 × 10^{-8} Torr of C_2D_4: (a) isolation of $(C_2H_5)(CH_3)SiH^+$ (m/z 73), formed by electron impact ionization of (C_2H_5)-$(CH_3)SiH_2$ (pulsed into the vacuum chamber; (b) 1.0-s reaction with C_2D_4; (c) 2.5-s reaction with C_2D_4; (d) 5.0-s reaction with C_2D_4. The peaks at m/z ratio 105–111 are due to simple adduct formation with ethene-d_4.

of the exchange processes (reactions 7 and 8) suggests no significant barriers for the exchange mechanism (process 10).[36] The ethene insertion/β-hydrogen migration process (reaction 10) accounts for the inert behavior of the methyl groups of $(CH_3)_2SiH^+$ and $(C_2H_5)(CH_3)SiH^+$ toward labeled ethene.

By analogy to process 10, $(CH_3)SiH_2^+$ should yield two exchangeable hydrogens with ethene-d_4. Surprisingly, all five hydrogens are exchangeable for $(CH_3)SiH_2^+$ with ethene-d_4 (process 11) (k_{obsd} = [1.1(0.3)] × 10^{-9} cm^3

$$(CH_3)SiH_2^+ \xrightarrow{C_2D_4} (CD_3)SiD_2^+ \qquad (11)$$

$molecule^{-1}$ s^{-1}; eff = 1.0). Figure 5 illustrates the mass spectra obtained at various reaction times. Double resonance[9,10] confirms that multiple H/D exchange dominates over a single H/D exchange per collision, and this is in accord with the spectra in Figure 5. Authentic $(CH_3)SiD_2^+$ (formed by EI of $(CH_3)SiD_3$) undergoes facile exchange of the three methyl hydrogens (process 12) (k_{obsd}

(30) (a) Rogers, D. S.; Walker, K. L.; Ring, M. A.; O'Neal, H. E. *Organometallics* **1987**, *6*, 2313. (b) Dickinson, A. P.; Nares, K. E.; Ring, M. A.; O'Neal, H. E. *Organometallics* **1987**, *6*, 2596.

(31) Welsh, K. M.; Michl, J.; West, R. *J. Am. Chem. Soc.* **1988**, *110*, 6689.

(32) Gaspar, P. P. *Reactive Intermediates*; Jones, M. J., Moss, R. A., Eds.; Wiley: New York, 1978; Vol. 3, p 333.

(33) Collman, J. P.; Hegedus, L. S. *Principles and Applications of Organotransition Metal Chemistry*; University Science Books: Mill Valley, CA, 1980; p 292.

(34) Hajdasz, D.; Squires, R. R. *J. Chem. Soc., Chem. Commun.* **1988**, 1212.

(35) Li, X.; Stone, J. A. *J. Am. Chem. Soc.* **1989**, *111*, 5586.

(36) (a) Grabowski, J. J.; DePuy, C. H.; Van Doren, J. M.; Bierbaum, V. M. *J. Am. Chem. Soc.* **1985**, *107*, 7384 and references cited therein. (b) Moylan, C. R.; Brauman, J. I. *Annu. Rev. Phys. Chem.* **1983**, *34*, 187. (c) Jasinski, J. M.; Brauman, J. I. *J. Am. Chem. Soc.* **1980**, *102*, 2906. (d) Ausloos, P.; Lias, S. G. *J. Am. Chem. Soc.* **1981**, *103*, 3641. (e) Hunter, E. P.; Lias, S. G. *J. Phys. Chem.* **1982**, *86*, 2769. (f) Olmstead, W. N.; Brauman, J. I. *J. Am. Chem. Soc.* **1977**, *99*, 4219.

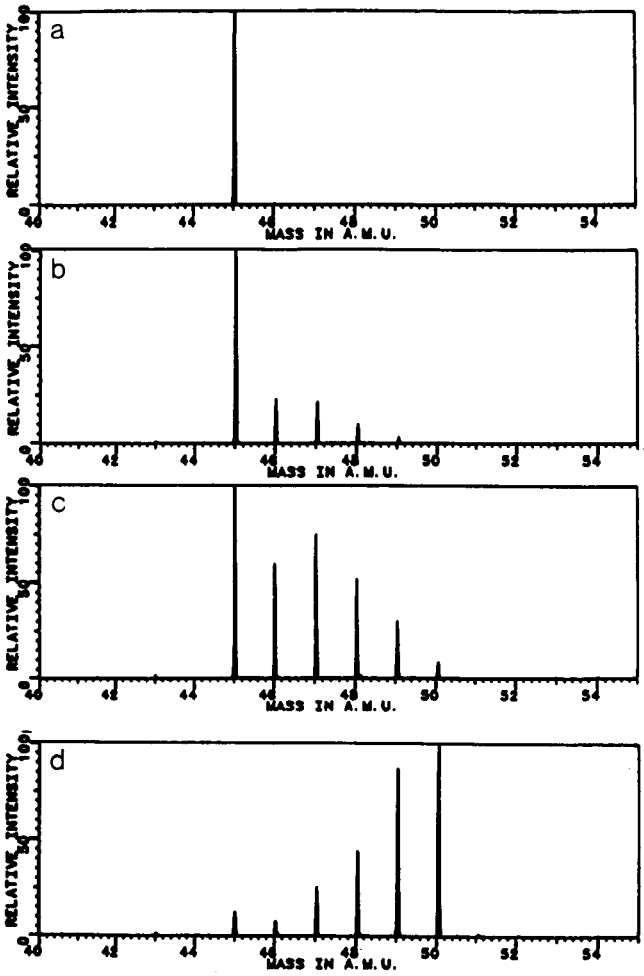

Figure 5. Mass spectra for reaction of $(CH_3)SiH_2^+$ with 2.6 × 10^{-8} Torr of C_2D_4: (a) isolation of $(CH_3)SiH_2^+$, formed by electron impact ionization of $(CH_3)SiH_3$ (pulsed into the vacuum chamber); (b) 0.5-s reaction with C_2D_4; (c) 1.25-s reaction with C_2D_4; (d) 5.0-s reaction with C_2D_4.

$$(CH_3)SiD_2^+ \xrightarrow{C_2D_4} (CD_3)SiD_2^+ \qquad (12)$$

= [5.6(1.7)] × 10^{-10} cm^3 $molecule^{-1}$ s^{-1}; eff = 0.52). H/D exchange (processes 11 and 12) may proceed by two distinct mechanisms, one where the silyl hydrogens are exchanged (presumably by process 10) and another where the methyl hydrogens are exchanged. One possible explanation for the exchange of the methyl hydrogens for $(CH_3)SiH_2^+$ is interconversion of a silylenium ion with an α-silyl-substituted carbenium ion by reversible 1,2-hydrogen migration (process 13), resulting in equilibration of the

$$(CH_3)SiH_2^+ \rightleftharpoons {}^+CH_2\text{–}SiH_3 \qquad (13)$$

hydrogen atoms. Hopkinson and Lien, using ab initio theory, found that the silylenium ion ($(CH_3)SiH_2^+$) is ca. 40 kcal/mol more stable than the corresponding carbenium ion ($^+CH_2$–SiH_3) and that there is little or no barrier in excess of the overall endothermicity for their interconversion.[37] It is possible that ethene coordination provides sufficient energy to drive this interconversion (process 13). This process, however, seems unlikely on two accounts. First, ethene binding energy to $(CH_3)_3Si^+$ is between 20 and 25 kcal/mol,[34,35] much less than that required to drive process 13. Second, ethene coordination to $(CH_3)_2SiH^+$ does not result in silyl hydrogen/methyl hydrogen scrambling (vide supra). Consequently, it appears that two distinct mechanisms are involved in the H/D exchange process (reaction 11), one where the silyl hydrogens are exchanged (presumably process 10) and one where the methyl hydrogens are exchanged.

(37) Hopkinson, A. C.; Lien, M. H. *J. Org. Chem.* **1981**, *46*, 998.

Scheme I

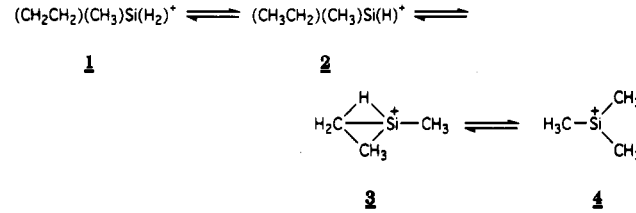

Further insight into the H/D exchange process for reaction 11 is obtained by observing *facile* isotopic carbon atom exchange between $(CH_3)SiH_2^+$ and ethene-$^{13}C_2$ (process 14) (k_{obsd} = [8.2(2.5)] × 10^{-10} cm^3 $molecule^{-1}$ s^{-1}, eff = 0.72). In contrast, there is *no* isotopic exchange

$$(CH_3)SiH_2^+ + {}^{13}C_2H_4 \rightarrow ({}^{13}CH_3)SiH_2^+ + C^{13}CH_4 \qquad (14)$$

between $(CH_3)_2SiH^+$ and ethene-$^{13}C_2$. The high efficiency of processes 11 and 14 (essentially unit efficiency accounting for statistical factors) implies a mechanism with no significant barriers for silylmethyl/ethene isotopic exchange.[36] In contrast, there is a prohibitive barrier for carbon atom scrambling between ethene and the methyl groups for the ethene–($(CH_3)_2SiH^+$) collision complex. Both silylenium ions, $(CH_3)SiH_2^+$ and $(CH_3)_2SiH^+$, have qualitatively similar stereoelectronic properties, yet there is a dramatic difference in their reactions with labeled ethene. Therefore, a mechanism must account for the pronounced difference in reactivity of these silylenium ions with labeled ethene that does not invoke differences in stereoelectronic properties. We now consider a mechanism for isotopic exchange in processes 12 and 14.

Proposed Mechanism for Processes 12 and 14. A proposed mechanism for the exchange processes (reactions 12 and 14) is presented in Scheme I. Initially, ethene coordination yields 1, which is activated by the ethene–silylenium ion binding energy (ca. 20–25 kcal/mol).[34,35] Facile, reversible ethene insertion/β-hydrogen migration interconverts 1 and 2 (e.g., process 10).[28-32] We estimate that 2 is about 30 kcal/mol more stable than 1 (Table I); consequently, the collision complex will predominantly exist as 2 instead of 1. We propose that activated 2 rearranges to 4 via a concerted 1,2-hydrogen/1,2-methyl migration. The conversion of 2 to 4 is exothermic by ca. 20 kcal/mol (Table I).[22,23] Highly activated 4 subsequently decomposes by the reverse process with ethene extrusion. Scheme I accounts for the Si–methyl/ethene isotopic scrambling observed for reactions 11, 12, and 14.

Reactions involving intramolecular positional interchange of σ-bonded groups (e.g., Scheme I) are called "dyotropic" processes.[8] There are several examples of dyotropic processes that involve 1,2-interchanges.[8,38-40] We envision that the dyotropic rearrangement (transition state 3) involves a thermally allowed [$\sigma_s^2 + \sigma_a^2$] process (Figure 6). Such a transition state is not sterically constrained, and the involvement of d orbitals or the empty p orbital

(38) (a) Gell, K. I.; Williams, G. M.; Schwartz, J. *J. Chem. Soc., Chem. Commun.* **1980**, 550. (b) Erker, G. *Acc. Chem. Res.* **1984**, *17*, 103.
(39) Wayland, B. B.; Feng, Y.; Ba, S. *Organometallics* **1989**, *8*, 1438.
(40) Yokelson, H. B.; Siegel, D. A.; Millevolte, A. J.; Maxka, J.; West, R. *Organometallics* **1990**, *9*, 1005.

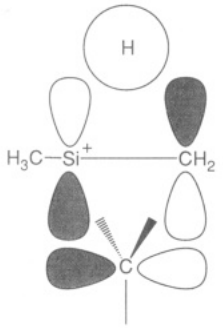

Figure 6. Orbital representation of the transition state **3** for dyotropic rearrangement.

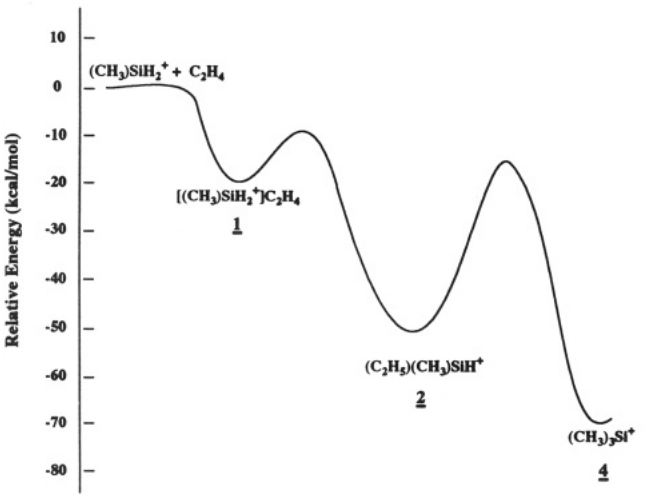

Figure 7. Potential energy surface for Scheme I. Thermochemical values for distinct intermediates are from Table I.

on the silicon atom is not required. Gas-phase kinetic studies have found that (chloromethyl)dimethylsilane undergoes the thermal rearrangement shown in process 15.[41,42] This unimolecular rearrangement is viewed as

$$(CH_3)_2(CH_2Cl)SiH \rightarrow (CH_3)_3SiCl \qquad (15)$$

dyotropic, involving concerted 1,2-hydrogen/1,2-chloro migration.[43] A potential energy surface for Scheme I is presented in Figure 7. Thermochemical values for distinct intermediates are obtained from Table I, and barriers for rearrangements are simply estimates. We believe that there is a low barrier (ca. 10 kcal/mol) for ethene insertion into the Si–H bond (process 10; vide supra). The transition state for conversion of **2** to **4** (Figure 6) is highly ordered and, consequently, is assigned a barrier of ca, 35 kcal/mol. This barrier height is still ca. 15 kcal/mol below the asymptotic energy limit (Figure 7). Although the barrier for conversion of **2** to **4** is high (ca. 35 kcal/mol), the barrier for conversion of **2** back to **1** is also high (ca. 40 kcal/mol). Consequently, **2** has a high probability for conversion to **4** as required by the kinetics.

We now consider the analagous dyotropic rearrangement for $(C_2H_5)(CH_3)_2Si^+$, formed by reaction of $(CH_3)_2SiH^+$ with ethene. The corresponding dyotropic rearrangement

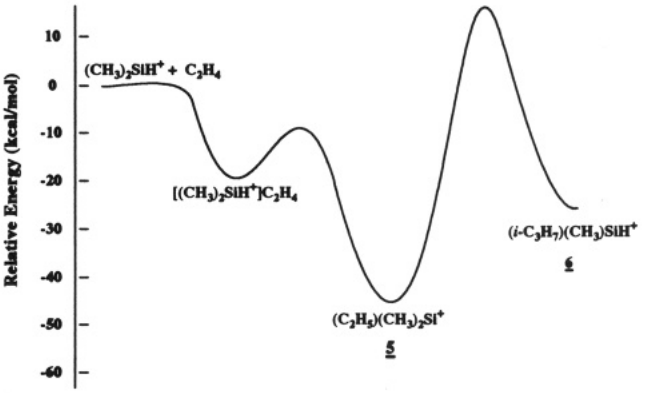

Figure 8. Potential energy surface for dyotropic rearrangement of $(C_2H_5)(CH_3)_2Si^+$ and $(i\text{-}C_3H_7)(CH_3)SiH^+$. Thermochemical values for distinct intermediates are from Table I.

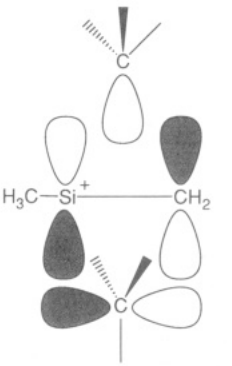

Figure 9. Orbital representation of the transition state for the degenerative dyotropic migration of $(C_2H_5)(CH_3)_2Si^+$ (process 17).

would interconvert $(C_2H_5)(CH_3)_2Si^+$ (**5**) and $(i\text{-}C_3H_7)(CH_3)SiH^+$ (**6**) (process 16). A potential energy surface

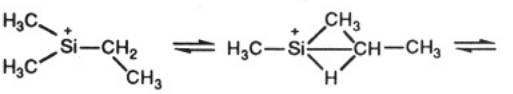

5

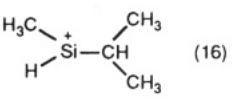

(16)

6

for this process is depicted in Figure 8, starting with ethene reacting with $(CH_3)_2SiH^+$, and thermochemical values for the distinct intermediates are obtained from Table I. The barrier for conversion of **6** to **5** is estimated to be ca. 35 kcal/mol, analogous to that for conversion of **2** to **4**. This energy barrier exceeds the asymptotic energy limit by ca. 10 kcal/mol, and consequently, this dyotropic rearrangement is not energetically feasible. Another possible rearrangement for $(C_2H_5)(CH_3)_2Si^+$ (**5**) involves concerted 1,2-dimethyl migrations (dyotropic rearrangement) (process 17). This rearrangement could proceed in a fashion

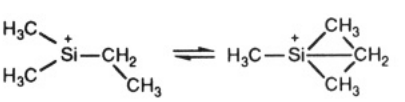

(17)

5

analogous to that for $(C_2H_5)(CH_3)SiH^+$ (**2**; Figure 6). In this case, one methyl migrates with retention of configuration and one with inversion (Figure 9). Absence of silylmethyl group scrambling (process 7) implies a *pro-*

(41) Martin, J. G.; Ring, M. A.; O'Neal, H. E. *Organometallics* **1986**, *5*, 1228.
(42) Davidson, I. M. T.; Ijadi-Maghsoodi, S. *Organometallics* **1986**, *5*, 1086.
(43) Clarke, M. P.; Damrauer, R.; Davidson, I. M. T.; Simon, R. *Organometallics* **1989**, *8*, 2031.
(44) Auxiliary thermochemical information from: Lias, S. G.; Bartmess, J. E.; Liebman, J. F.; Holmes, J. L.; Levin, R. D.; Mallard, W. G. *J. Phys. Chem. Ref. Data, Suppl. 1* **1988**, *17*.

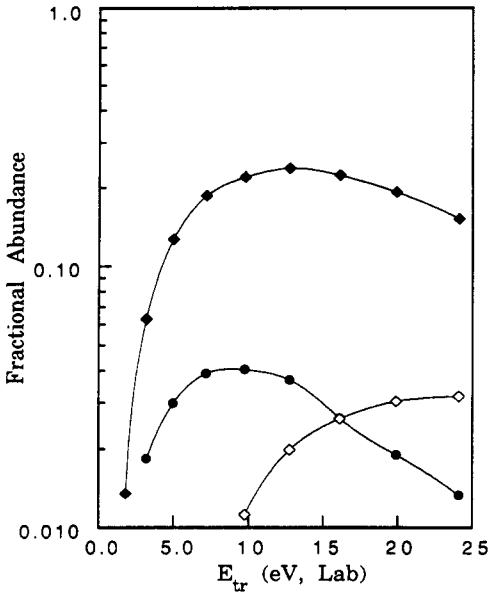

Figure 10. Variation of fractional fragment ion abundances as a function of kinetic energy (laboratory frame) for "on-resonance" irradiation for CAD of $(^{13}C_2H_5)(CH_3)SiH^+$ (trapping voltage 1.2 V): (◆) CH_5Si^+; (●) $^{13}CH_5Si^+$; (◇) CH_3Si^+.

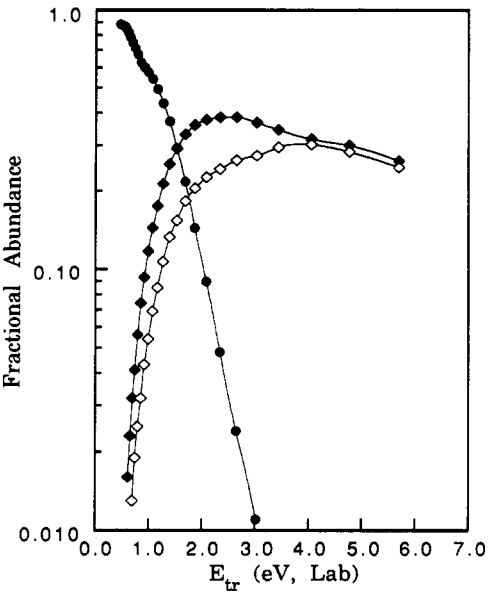

Figure 11. Variation of fraction ion abundances as a function of maximum kinetic energy (calculated directly from eq 5) for SORI-CAD (500 ms duration pulse, 1.02 V electric field, trapping voltage 1.2 V) of $(^{13}C_2H_5)(CH_3)SiH^+$ formed in reaction 8: (●) $(^{13}C_2H_5)(CH_3)SiH^+$; (◇) CH_5Si^+; (◆) $^{13}CH_5Si^+$.

hibitive (>50 kcal/mol) barrier for process 17 (the excess energy of $(C_2H_5)CH_3)_2Si^+$ (**5**) is ca. 43 kcal/mol; Figure 8). It is not surprising that 1,2-dimethyl migrations (process 17) would have a larger barrier than that for the conversion of **2** to **4** (ca. 35 kcal/mol) due to a more constrained transition state (Figure 9).

The above interpretation explains the different behavior of the various methylsilylenium ions with isotopically labeled ethene without invoking unique stereoelectronic arguments. The silyl H in an activated ethylsilylenium ion is the key to rearrangement by dyotropic migration (Scheme I) and has origins in the thermodynamic stability of distinct intermediates and barrier heights for rearrangement.

CAD of Isotopically Labeled Silylenium Ions. CAD of isotopically labeled silylenium ions provides additional information concerning scrambling processes prior to dissociation. A particularly interesting species to consider is CAD of $(^{13}C_2H_5)(CH_3)SiH^+$, formed in reaction 8. The CAD breakdown curve for this ion is presented in Figure 10. The most significant feature is the isotopic distribution for ethene elimination. As seen in Figure 10, the fraction of ethene elimination as $C^{13}CH_4$ is highest at low kinetic energy and steadily decreases as kinetic energy increases. Elimination of ethene as the mixed isotopolog requires carbon atom scrambling, presumably by Scheme I (process 18). At high energy, however, direct elimination of ethene

$$(C_2H_5)(CH_3)SiH^+ \rightleftharpoons (CH_3)_3Si^+ \qquad (18)$$

by β-hydrogen atom migration is favored over the rearrangement process. CAD by "off-resonance" irradiation was also examined in order to facilitate isotopic scrambling prior to fragmentation. The variation of ethene isotopolog eliminations as a function of kinetic energy for SORI-CAD of $(^{13}C_2H_5)(CH_3)SiH^+$, formed by reaction 8, is illustrated in Figure 11. At low collision energy, the $C^{13}CH_4/^{13}C_2H_4$ elimination ratio is essentially 2 (i.e., a statistical isotopic distribution). This result indicates that the three carbon atoms are equilibrated prior to fragmentation. As the collision energy increases, this ratio decreases, indicating a lower degree of scrambling prior to dissociation. In contrast, CAD of $(^{13}C_2H_5)(CH_3)_2Si^+$, formed by ethene displacement of $(C_2H_5)(CH_3)_2Si^+$ by ethene-$^{13}C_2$, results in ethene elimination exclusively as $^{13}C_2H_4$ (process 19), even with an "off-resonance" irradiation pulse for CAD.[7] Absence of scrambling for process 19 is consistent with observation of an exclusive *single* H/D exchange for reaction 7 as well as with the potential energy surface presented in Figure 8. The SORI-CAD results for $(^{13}C_2H_5)(CH_3)SiH^+$ clearly indicate that isotopic scrambling, presumably by process 18, has a lower energy requirement than the corresponding elimination of ethene.

$$(^{13}C_2H_5)(CH_3)_2Si^+ \rightarrow (CH_3)_2SiH^+ + {}^{13}C_2H_4 \qquad (19)$$

Finally, CAD of $(CH_3)_2SiH^+$ and $(CH_3)_2SiD^+$ were investigated. The CAD breakdown curves for each isotopolog are presented in Figures 12 and 13. The dominant fragmentation channel is ethene extrusion with additional losses observed at higher collision energy. In the case of $(CH_3)_2SiD^+$, ethene elimination occurs as both C_2H_4 and C_2H_3D with elimination of $C_2H_3D^+$ dominating (Figure 13). SORI-CAD of $(CH_3)_2SiD^+$ is illustrated in Figure 14 and yields both dehydrogenation (H_2 and HD losses) and ethene elimination. At low collision energy the C_2H_4:C_2H_3D ratio is ca. 1:2.2 (Figure 14). A statistical distribution would yield a C_2H_4:C_2H_3D ratio of 1:1.3; hence, elimination of ethene as C_2H_3D is favored over a statistical isotopolog distribution at low kinetic energy. These results suggest that ethene elimination for activated $(CH_3)_2SiH^+$ involves prior rearrangement to $(C_2H_5)SiH_2^+$, presumably by dyotropic migration analogous to Scheme I. Reversible β-hydrogen migration/olefin insertion may occur prior to ethene elimination. The high abundance of ethene elimination as C_2H_3D may be due to kinetic isotope effects, which would be maximized at the low internal energies involved in fragmentation by "off-resonance" irradiation.

Additional insight into the mechanism for ethene elimination for CAD of $(CH_3)_2SiH^+$ can be obtained by studying both CAD of $(C_2H_5)SiH_2^+$ and the reaction of SiH_3^+ with ethene. CAD of $(C_2H_5)SiH_2^+$, "on-resonance"

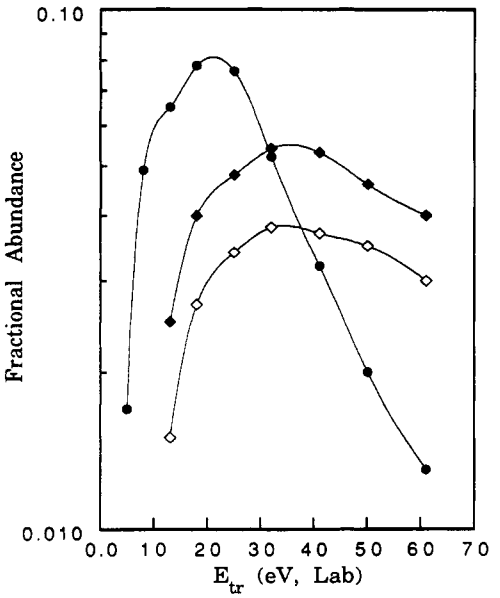

Figure 12. Variation of fractional fragment ion abundances as a function of kinetic energy (laboratory frame) for "on-resonance" irradiation for CAD of $(CH_3)_2SiH^+$ (trapping voltage 2.0 V): (●) SiH_3^+; (◇) SiH^+; (◆) Si^+.

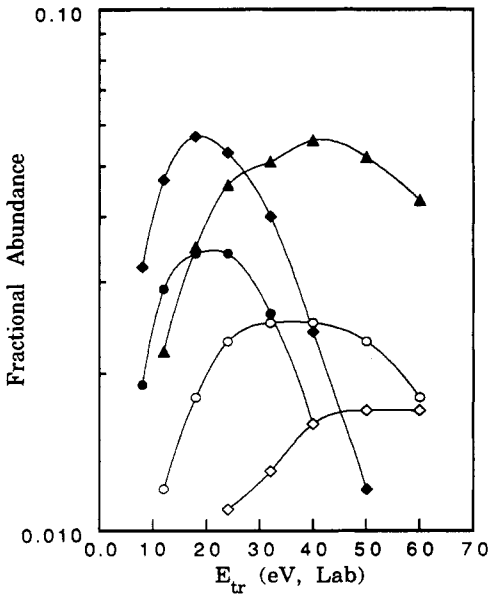

Figure 13. Variation of fractional fragment ion abundances as a function of kinetic energy (laboratory frame) for "on-resonance" irradiation for CAD of $(CH_3)_2SiD^+$ (trapping voltage 2.0 V): (●) SiH_2D^+; (◆) SiH_3^+; (▲) SiH^+; (○) SiD^+; (◇) Si^+.

irradiation, yields predominant ethene elimination with only a trace of dehydrogenation, in accord with that for $(CH_3)_2SiH^+$. SORI-CAD of $(C_2H_5)SiH_2^+$ yields significant amounts of both dehydrogenation and ethene elimination, similar to that for SORI-CAD of $(CH_3)_2SiD^+$ (Figure 14). In addition, SiH_3^+ reacts with ethene to yield exclusive dehydrogenation (k = [4.8(1.4)] × 10^{-10} cm^3 $molecule^{-1}$ s^{-1}, eff = 0.38) (reaction 20). Multiple H/D exchange is

$$SiH_3^+ + C_2H_4 \rightarrow C_2H_5Si^+ + H_2 \qquad (20)$$

competitive with dehydrogenation for reaction of SiH_3^+ with ethene-d_4. The predominance of ethene elimination over dehydrogenation for "on-resonance" irradiation for CAD of $(C_2H_5)SiH_2^+$ indicates that ethene elimination is kinetically favored. Observation of dehydrogenation for

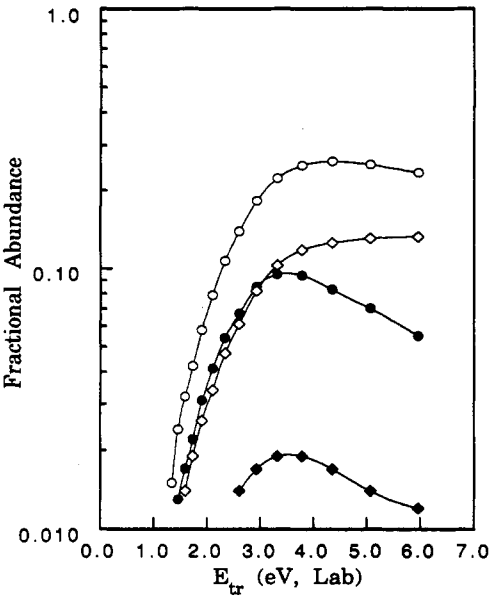

Figure 14. Variation of fractional fragment ion abundances as a function of maximum kinetic energy (calculated directly for eq 5) for SORI-CAD (500 ms duration pulse, 1.02 V electric field, trapping voltage 2.0 V) of $(CH_3)_2SiD^+$: (●) $C_2H_4DSi^+$; (◆) $C_2H_5Si^+$; (◇) SiH_2D^+; (○) SiH_3^+.

SORI-CAD of $(C_2H_5)SiH_2^+$ and reaction 20 provide additional support for the interconversion of activated $(CH_3)_2SiH^+$ and $(C_2H_5)SiH_2^+$.

Conclusions

The lowest energy pathway for dissociation of $(CH_3)_3Si^+$ (4) and $(C_2H_5)(CH_3)SiH^+$ (2) is ethene elimination. The elimination of ethene from activated 4 does not proceed by simple extension of vibrations (process 3). Instead, CAD combined with isotopic exchange reactions suggests that 2 and 4 readily interconvert upon activation. This interconversion is proposed to involve a concerted 1,2-hydrogen/1,2-methyl migration (dyotropic rearrangement, Scheme I). We envision that the dyotropic rearrangement proceeds by a thermally allowed [$\sigma_s^2 + \sigma_a^2$] process (Figure 6). Hence, ethene elimination from activated 4 involves initial rearrangement to 2 with subsequent β-hydrogen migration and ethene extrusion (Scheme I). A potential energy surface for ethene elimination from activated 4 is presented in Figure 6. The key process in Figure 6 is the barrier for rearrangement of 4 to 2 (transition state 3), which is believed to be substantial (ca. 55 kcal/mol). The corresponding silylenium ion, $(CH_3)_2SiH^+$, appears to decompose by a process analogous to that for 4 (Scheme I) with initial conversion to $(C_2H_5)SiH_2^+$ followed by decomposition (either by ethene elimination or by dehydrogenation).

Activated $(C_2H_5)(CH_3)_2Si^+$ decomposes by direct ethene elimination (β-hydrogen migration/ethene extrusion). This was confirmed by observation of exclusive elimination of ethene-$^{13}C_2$ for CAD of $(^{13}C_2H_5)(CH_3)_2Si^+$.[7] Absence of scrambling for ethene elimination in this case is believed to be the result of prohibitive barriers for dyotropic migration, either by process 16 (Figure 8) or by process 17.

Acknowledgment is made to the National Science Foundation NSF-EPSCoR (Grant RII-861075), the Society for Analytical Chemists of Pittsburgh, and VG Corp. for partial support of this research.

OM920549+